Scientia Iranica D (2015) 22(3), 1077–1084

Sharif University of Technology
Scientia Iranica
Transactions D: Computer Science & Engineering and Electrical Engineering
www.scientiairanica.com

Research Note

An analysis on the main formulas of Z-source inverter

M. Shid Pilehvar, M. Mardaneh* and A. Rajaei

Department of Electrical and Electronics Engineering, Shiraz University of Technology, Shiraz, Iran.

Received 7 November 2013; received in revised form 15 December 2014; accepted 13 April 2015

KEYWORDS
Z-source inverter;
Voltage stress;
Current ripple;
Switching loss;
Switching device power.

Abstract. This paper proposes an analysis of the calculation of voltage and current ripples, voltage stresses, switching device power, and switching loss in the Z-source inverter. In this paper, the formulas of the inductor current ripple, capacitor voltage ripple, voltage stress on the devices and capacitors, switching device power and switching loss, are presented. Computing these formulas will help us greatly in the performance improvement of the Z-source inverter, and in this paper, a detailed analysis of the main formulas is presented. Simulation results are also given to confirm the analysis.

1. Introduction

The Voltage Source Inverter (VSI) and the Current Source Inverter (CSI) are two traditional types of inverter. For the VSI, a dc voltage source paralleled with a large capacitor feeds a three-phase bridge (consisting of six switches). This dc voltage source can be a battery, fuel cell or solar cell. For the CSI, a dc current source feeds a three-phase bridge (consisting of six switches). This dc current source can be a large inductor which is fed from a battery, fuel cell or solar cell. Despite widespread use, these two traditional inverters have problems. For example, for the VSI, the ac output voltage is lower than the input dc voltage, thus, it can only perform a buck dc-ac power conversion. On the other hand, for the CSI, the ac output voltage is greater than the input dc voltage, thus, presenting a voltage boost dc-ac power conversion. Therefore, in applications where both voltage buck and boost are needed, an additional dc-dc converter should be placed before both VSI and CSI, which significantly increases the complexity and cost of the system. To overcome this problem, and many other problems of traditional inverters, in 2002, the topology of the Z-source inverter [1] was proposed by Peng.

Unlike other inverters, the Z-source inverter can provide shoot-through states to boost the input dc voltage when both switches in the same phase leg are on, and, because of this feature, the reliability of the inverter is greatly improved. In comparison to traditional inverters, the Z-source inverter is more reliable, has lower costs and higher efficiency [2].

In recent years, the Z-source inverter has received wide attention in research and industrial applications, including motor drives [3], photovoltaic systems [4,5] and the traction drive of fuel cell-battery hybrid electric vehicles [6]. Besides, some investigations have also presented new methods for performance improvement of the Z-source inverter, such as reduction of Z-source capacitor voltage stress [7], minimization of inductor current ripple [8,9], and improvement of voltage boost ability [10]. In this paper, an analysis of the main formulas of the Z-source inverter is proposed. For this purpose, the formulas of the inductor current ripple, capacitor voltage ripple, voltage stress on the devices and capacitors, switching device power and switching loss, are calculated. Simulation results are also presented to validate the analysis.

*. *Corresponding author. Tel.: +98 71 37264121; Fax: +98 71 37353502*
E-mail address: mardaneh@sutech.ac.ir (M. Mardaneh)

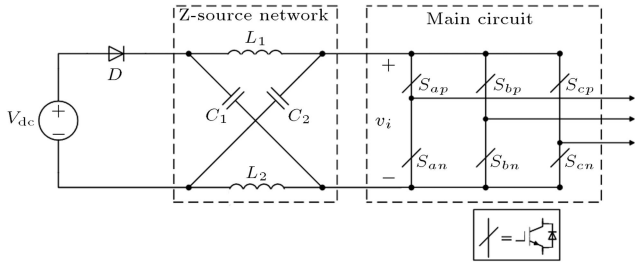

Figure 1. Configuration of Z-source inverter.

2. Operation principle of Z-source inverter

Figure 1 shows the structure of the Z-source inverter. The Z-source inverter operates in two modes: the shoot-through state and non-shoot-through state. In the shoot-through state, both switches of the same phase leg are on, simultaneously, and, in a non-shoot-through state, the upper switch of a phase leg and the lower switch of another phase leg are connected, simultaneously.

As analyzed in [1], If the capacitors and inductors of the Z-source impedance network have the same capacitance and inductance ($C_1 = C_2 = C$ and $L_1 = L_2 = L$), respectively, the maximum value of the Z-source impedance output voltage can be calculated as follows:

$$\hat{v}_i = V_C - v_L = 2V_C - V_{\rm dc} = \frac{T_{sw}}{T_1 - T_0} V_{\rm dc} = BV_{\rm dc}, \quad (1)$$

where B is the boost factor and can be obtained as follows:

$$B = \frac{T_{sw}}{T_1 - T_0} = \frac{1}{1 - 2(T_0/T_{sw})} = \frac{1}{1 - 2D} \geq 1, \quad (2)$$

where T_0 and T_1 are the total shoot-through state and total non-shoot-through state times, respectively, during one switching cycle, T_{sw}, and $T_{sw} = T_0 + T_1$. It should be noted that D is the shoot-through duty ratio, which is greater than, or equal to, zero, and less than, or equal to, 0.5, and can be obtained from T_0/T_{sw}.

The peak value of the fundamental output phase voltage can be expressed as:

$$(\hat{v}_o)_1 = \frac{M\hat{v}_i}{2}. \quad (3)$$

According to Eq. (1), Eq. (3) can be further expressed as:

$$(\hat{v}_o)_1 = \frac{\rm MBV_{dc}}{2}. \quad (4)$$

To control the Z-source inverter, all traditional pulsewidth modulations (PWM) can be used. But, when the dc source voltage is not large enough, a modified PWM with shoot-through states is needed to increase the voltage [1]. Figure 2 shows the proposed PWM for the Z-source inverter used in this study.

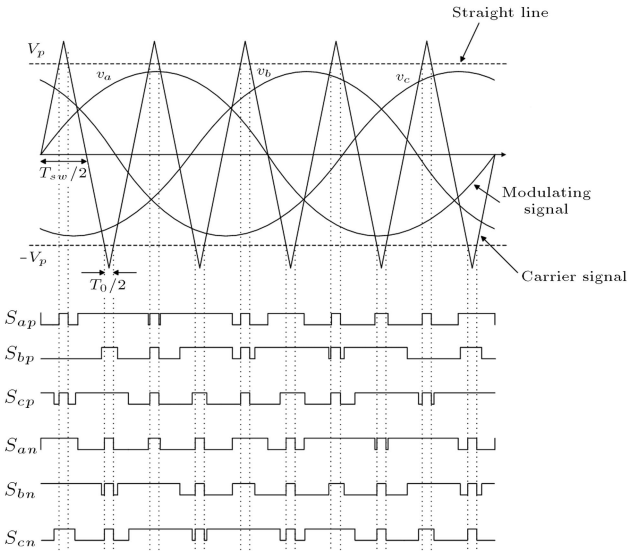

Figure 2. Waveforms and switching strategy of PWM control method for Z-source inverter, considering shoot-through states.

In this investigation, to control the shoot-through duty ratio and produce switching PWM pulses, a triangular carrier signal is compared with a sinusoidal modulating signal. Also, two straight lines are used as shoot-through reference lines, V_p and $-V_p$. As shown in Figure 2, whenever the triangular waveform is more than V_p or less than $-V_p$, the Z-source inverter operates in a shoot-through state. It should be noted that V_p is equal or greater than the peak value of the modulating signals, and, in this study, the frequency of the modulating signals is taken as 60 Hz.

3. Voltage stresses

3.1. Z-source capacitor voltage stress

As analyzed in [1], the capacitor voltage of the Z-source impedance network can be calculated as follows:

$$V_{C1} = V_{C2} = V_C = \left(\frac{1 - T_0/T_{sw}}{1 - 2T_0/T_{sw}}\right) V_{\rm dc}$$

$$= \frac{1 - D}{1 - 2D} V_{\rm dc}. \quad (5)$$

From Eqs. (2) and (5), the Z-source capacitor voltage can be further expressed as:

$$V_c = \frac{B + 1}{2B} BV_{\rm dc} = \frac{B + 1}{2} V_{\rm dc}. \quad (6)$$

Therefore, from Eq. (6), V_C increases by enhancing B or $V_{\rm dc}$.

As shown in Figure 3, the boost factor can be controlled by the values of straight lines, as follows:

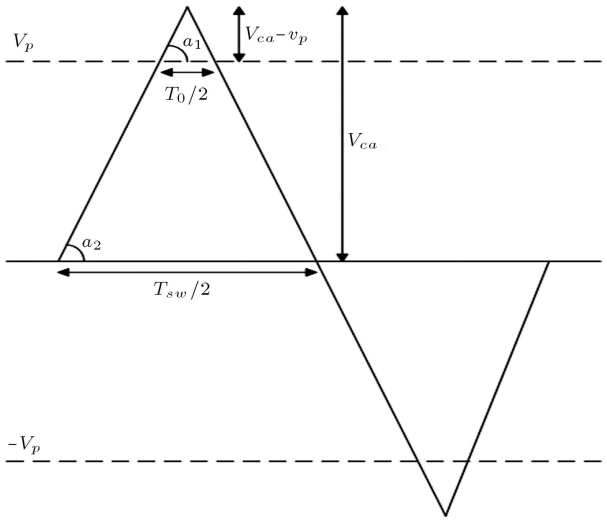

Figure 3. Triangular carrier signal and two straight lines in one switching cycle.

$$\tan a_1 = \frac{V_{ca} - V_p}{T_0/4}, \tag{7}$$

and:

$$\tan a_2 = \frac{V_{ca}}{T_{sw}/4}, \tag{8}$$

where V_{ca} is the peak value of the triangular carrier signal.

According to Figure 3, since angle a_1 is equal to angle a_2, the shoot-through duty ratio can be calculated from Eqs. (7) and (8), as shown below:

$$\frac{T_0}{T_{sw}} = \frac{V_{ca} - V_p}{V_{ca}} = D. \tag{9}$$

By substituting Eq. (9) into Eq. (2), the boost factor can be expressed as:

$$B = \frac{1}{1 - 2\left(\frac{V_{ca}-V_p}{V_{ca}}\right)}. \tag{10}$$

According to Eqs. (9) and (10), when V_{ca} is constant and V_p is increased, D and B are reduced. In such circumstances, from Eq. (6), V_C will decrease.

The Z-source capacitor voltage can be considered as the voltage stress across the capacitors, S_C, and, from Eqs. (6) and (10), it can be further determined by the following relation:

$$S_C = V_c = \frac{V_p}{2V_p - V_{ca}} V_{\rm dc}. \tag{11}$$

As can be derived from Eq. (11), V_p cannot be less than $V_{ca}/2$. Also, if $V_p = V_{ca}/2$, V_C goes to infinity, then, a high Z-source capacitor voltage stress is presented.

3.2. Voltage stress across the devices

According to Eq. (1), the voltage stress across the switches, S_S, can be expressed as:

$$S_S = \hat{v}_i = BV_{\rm dc}. \tag{12}$$

From Eqs. (2) and (12), it can be concluded that:

$$S_S = \frac{1}{1 - 2\left(\frac{V_{ca}-V_p}{V_{ca}}\right)} V_{\rm dc} = \frac{V_{ca}}{2V_p - V_{ca}} V_{\rm dc}. \tag{13}$$

As can be derived from Eq. (13), S_S increases by enhancing $V_{\rm dc}$ and decreases by enhancing V_p. Also, if $V_p = V_{ca}/2$, S_S goes to infinity, this may damage the switching devices, because of the limitation of their voltage rating.

4. Current and voltage ripples

4.1. Z-source inductor current ripple

As previously mentioned, during the shoot-through state, the inductors are charged by the capacitors. Therefore, the Z-source inductor current ripple can be expressed as:

$$\Delta i_L = \frac{T_0 V_C}{L} = \frac{DT_{sw} V_C}{L}. \tag{14}$$

From Eqs. (2), (6) and (14), it can be concluded that:

$$\Delta i_L = \frac{B^2 - 1}{4B} \frac{T_{sw} V_{\rm dc}}{L}. \tag{15}$$

As can be derived from Eq. (15), Δi_L increases by enhancing T_{sw} or $V_{\rm dc}$ and decreases by enhancing L. Also, if $B = 1$ or $D = 0$, Δi_L is equal to zero.

By substituting Eq. (10) into Eq. (15), the Z-source inductor current ripple can be further expressed as:

$$\Delta i_L = \frac{V_{ca} V_p - V_p^2}{V_{ca}(2V_p - V_{ca})} \frac{T_{sw} V_{\rm dc}}{L}. \tag{16}$$

From Eq. (16), it can be concluded that changing V_p has a significant impact on Δi_L, so, if $V_p = V_{ca}/2$ or $D = 0.5$, then, Δi_L goes to infinity.

4.2. Z-source capacitor voltage ripple

As previously mentioned, during the shoot-through state, capacitors are discharged by the Z-source inductor current. Therefore, the voltage ripple across the capacitors can be expressed as:

$$\Delta V_C = \frac{T_0 I_L}{C} = \frac{DT_{sw} I_L}{C}. \tag{17}$$

By applying the steady-state analysis presented in [11], the average values of the Z-source inductor current and

load current can be obtained as follows:

$$I_L = \frac{1-D}{1-2D} I_l, \tag{18}$$

$$I_l = \frac{V_C}{R_l}. \tag{19}$$

From Eqs. (18) and (19), it can be concluded that:

$$\Delta V_C = \frac{D(1-D)}{1-2D}\frac{T_{sw} I_l}{C} = \frac{D(1-D)}{1-2D}\frac{T_{sw} V_C}{C R_l}. \tag{20}$$

Substituting Eq. (19) into Eq. (20) gives the following relation;

$$\Delta V_C = D\left(\frac{1-D}{1-2D}\right)^2 \frac{T_{sw} V_{\rm dc}}{C R_l}. \tag{21}$$

According to Eq. (2), Eq. (21) can be further expressed as:

$$\Delta V_c = \frac{(B+1)(B^2-1)}{8B}\frac{T_{sw} V_{\rm dc}}{C R_l}. \tag{22}$$

As can be derived from Eq. (22), ΔV_C increases by enhancing T_{sw} or $V_{\rm dc}$, and decreases by enhancing C. Also, if $B = 1$ or $D = 0$, then, ΔV_C is equal to zero.

By substituting Eq. (10) into Eq. (22), the Z-source capacitor voltage ripple can be further expressed as:

$$\Delta V_c = \frac{V_p(V_p V_{ca} - V_p^2)}{V_{ca}(2V_p - V_{ca})^2}\frac{T_{sw} V_{\rm dc}}{C R_l}. \tag{23}$$

From Eq. (23), it can be concluded that changing V_p has a significant impact on ΔV_C. Also, if $V_p = V_{ca}/2$ or $D = 0.5$, then ΔV_C goes to infinity.

5. Total switching device power

Each switching device of the Z-source inverter should be selected according to the peak and average current impressed and the maximum voltage on it. For this purpose, the Switching Device Power (SDP) for each switch is introduced. The total SDP of the Z-source inverter is equal to the sum of SDP of all the switching devices used in the circuit. Actually, total SDP is a measure to choose the appropriate semiconductor devices, and thus, an important cost indicator of the Z-source inverter, whose average and peak are given by:

$$\text{Total average SDP} = (\overline{\text{SDP}})_t = \sum_{k=1}^{n} \hat{v}_{sk}\bar{i}_{sk}, \tag{24a}$$

$$\text{Total peak SDP} = (\hat{\text{SDP}})_t = \sum_{k=1}^{n} \hat{v}_{sk}\hat{i}_{sk}, \tag{24b}$$

where n is the number of switching devices used in the circuit. Also, $\bar{i}_{sk}$ and $\hat{i}_{sk}$ are the average and peak current through the kth switch, and $\hat{v}_{sk}$ is the peak voltage impressing the kth switch.

As previously mentioned, the current to the inverter bridge, i_i, consists of two elements. One is the current to the load during the non-shoot-through state and the other is the current through the switches during the shoot-through state. The current through the inverter during the shoot-through state is $2i_L$, and, because of the symmetry of the circuit, this current is evenly distributed in three parallel paths. Therefore, the average current through each switch of the inverter bridge during the shoot-through state can be expressed as:

$$I_{ss} = \frac{2\bar{i}_L}{3} = \frac{2I_L}{3}. \tag{25}$$

The peak fundamental output line current of the Z-source inverter can be calculated as:

$$(\hat{i}_o)_1 = \frac{2P_o}{3(\hat{v}_o)_1 \cos\varphi}, \tag{26}$$

where P_o is the output power of the Z-source inverter. Also, it is assumed that the load current of phase a is lagging by φ from its load voltage.

In the non-shoot-through state, from Eqs. (17) and (26), and since the line current is evenly shared by two switches in a line cycle, the average current through each switch is the same as conventional PWM inverters, and can be expressed as:

$$I_{sn} = \frac{2}{2\pi}(\hat{i}_o)_1 = \frac{2P_o}{3\pi(\hat{v}_o)_1 \cos\varphi} = \frac{4P_o}{3\pi \text{MBV}_{\rm dc}\cos\varphi}. \tag{27}$$

From Eqs. (25) and (27), the average current through each switch of the inverter bridge can be obtained as follows:

$$I_s = I_{ss}\frac{T_0}{T_{sw}} + I_{sn}\left(1 - \frac{T_0}{T_{sw}}\right)$$

$$= \frac{2}{3} I_L D + \frac{4P_o}{3\pi \text{MBV}_{\rm dc}\cos\varphi}(1-D). \tag{28}$$

From Eqs. (1), (24) and (28), the total average switching device power of the Z-source inverter can be calculated as follows:

$$\left(\overline{\text{SDP}}\right)_t = 6\hat{v}_i I_s = \frac{4D}{1-2D} I_L V_{\rm dc} + (1-D)\frac{8P_o}{\pi M\cos\varphi}. \tag{29}$$

According to Eqs. (2) and (29), it can be concluded that:

$$\left(\overline{\text{SDP}}\right)_t = 2(B-1) I_L V_{\rm dc} + \frac{(B+1)}{2B}\frac{8P_o}{\pi M\cos\varphi}. \tag{30}$$

According to Eqs. (10), (18), (19), and (30), the total

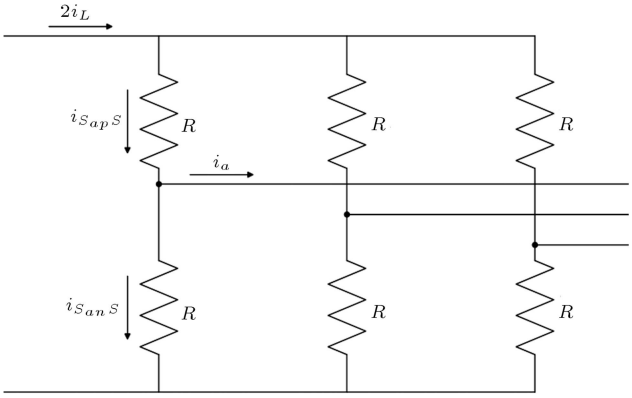

Figure 4. Model of the inverter bridge during shoot-through state.

average switching device power of the Z-source inverter can be further expressed as:

$$\left(\overline{\mathrm{SDP}}\right)_t = \frac{4V_p^2(V_{ca}-V_p)}{(2V_p-V_{ca})^3}\frac{V_{\mathrm{dc}}^2}{R_l} + \frac{V_p}{V_{ca}}\frac{8P_o}{\pi M\cos\varphi}. \quad (31)$$

To calculate the $(\hat{\mathrm{SDP}})_t$, both peak currents through the switches during shoot-through and non-shoot-through states are needed. As shown in Figure 4, if all switches have the same resistance during the shoot-through state, it can be concluded that:

$$\hat{i}_{S_{ap}s} = \frac{1}{2}i_a + \frac{2}{3}i_L. \quad (32)$$

By ignoring the Z-source inductor current ripple, when i_a is at its peak, the peak current through switch S_{ap} occurs, which can be obtained as follows:

$$\hat{i}_{S_{ap}s} = \frac{1}{2}\hat{i}_a + \frac{2}{3}I_L = \frac{1}{2}(\hat{i}_o)_1 + \frac{2}{3}I_L. \quad (33)$$

According to Eqs. (16), (26) and (33), the peak current through switch S_{ap} during the shoot-through state can be further determined by the following relation:

$$\hat{i}_{S_{ap}s} = \frac{P_o}{3(\hat{v}_o)_1\cos\varphi} + \frac{2}{3}I_L = \frac{2P_o}{3\mathrm{MB}V_{\mathrm{dc}}\cos\varphi} + \frac{2}{3}I_L. \quad (34)$$

Therefore, from Eqs. (1) and (34), the total peak switching device power of the Z-source inverter during the shoot-through state can be calculated as follows:

$$(\hat{\mathrm{SDP}})_{ts} = 6\hat{v}_i\hat{i}_{S_{ap}s} = \frac{4P_o}{3M\cos\varphi} + 4BI_LV_{\mathrm{dc}}. \quad (35)$$

From Eqs. (18), (19) and (35), the total peak switching device power of the Z-source inverter during the shoot-through state can be further expressed as:

$$(\hat{\mathrm{SDP}})_{ts} = \frac{4P_o}{3M\cos\varphi} + B(B+1)^2\frac{V_{\mathrm{dc}}^2}{R_l} = \frac{4P_o}{3M\cos\varphi} + \frac{4V_{ca}V_p^2}{(2V_p-V_{ca})^3}\frac{V_{\mathrm{dc}}^2}{R_l}. \quad (36)$$

On the other hand, the peak current through the switching devices during the non-shoot-through state is equal to the peak fundamental output line current of the Z-source inverter, and can be obtained as follows:

$$\hat{i}_{S_{ap}n} = (\hat{i}_o)_1 = \frac{2P_o}{3(\hat{v}_o)_1\cos\varphi}. \quad (37)$$

Therefore, from Eqs. (1), (17), and (37), the total peak switching device power of the Z-source inverter during the non-shoot-through state can be calculated as follows:

$$(\hat{\mathrm{SDP}})_{tn} = 6\hat{v}_i\hat{i}_{S_{ap}n} = \frac{8P_o}{M\cos\varphi}. \quad (38)$$

According to Eqs. (36) and (38), the total peak switching device power of the Z-source inverter can be expressed as:

$$(\hat{\mathrm{SDP}})_t = \max\left(\left(\hat{\mathrm{SDP}}\right)_{ts}, (\hat{\mathrm{SDP}})_{tn}\right) = \max\left(\frac{4P_o}{3M\cos\varphi} + \frac{4V_{ca}V_p^2}{(2V_p-V_{ca})^3}\frac{V_{\mathrm{dc}}^2}{R_l}, \frac{8P_o}{M\cos\varphi}\right). \quad (39)$$

The average input current from the dc source, I_{in}, is equal to the average current through the Z-source inductor, I_L. Therefore, by ignoring the total loss of the Z-source inverter, the input power from the dc source, P_{in}, is equal to the output power, P_o, and it can be concluded that:

$$I_{in} = I_L = \frac{P_o}{V_{\mathrm{dc}}}. \quad (40)$$

By substituting Eq. (40) into Eqs. (29) and (35), the total average and peak switching device powers of the Z-source inverter can be approximately calculated as follows:

$$(\overline{\mathrm{SDP}})_t \approx \frac{4(V_{ca}-V_p)}{2V_p-V_{ca}}P_o + \frac{V_p}{V_{ca}}\frac{8P_o}{\pi M\cos\varphi}, \quad (41)$$

$$(\hat{\mathrm{SDP}})_t \approx \max\left(\frac{4P_o}{3M\cos\varphi} + \frac{4V_{ca}}{2V_p-V_{ca}}P_o, \frac{8P_o}{M\cos\varphi}\right). \quad (42)$$

From Eqs. (41) and (42), the total average and peak Switching Device Power Ratios (SDPR) of the Z-source inverter can be expressed as:

$$(\mathrm{SDPR})_{av} = \frac{(\overline{\mathrm{SDP}})_t}{P_o} = \frac{4(V_{ca}-V_p)}{2V_p-V_{ca}} + \frac{V_p}{V_{ca}}\frac{8}{\pi M\cos\varphi}, \quad (43)$$

$$(\mathrm{SDPR})_{pk} = \frac{(\hat{\mathrm{SDP}})_t}{P_o} = \max\left(\frac{4}{3M\cos\varphi} + \frac{4V_{ca}}{2V_p-V_{ca}}, \frac{8}{M\cos\varphi}\right). \quad (44)$$

As can be derived from Eqs. (43) and (44), a change in parameters, such as V_p, M and φ, has a significant impact on $(\mathrm{SDPR})_{av}$and $(\mathrm{SDPR})_{pk}$.

6. Switching loss

Although high values of switching frequency, f_{sw}, cause low voltage and current ripples, they also increase the switching loss of the Z-source inverter. The switching loss of each IGBT during non-shoot-through and shoot-through states, P_{swn} and P_{sws}, are given by [2]:

$$P_{swn} = \frac{1}{2\pi T_{sw}} \left(E_{\text{swonn}} + E_{\text{swoffn}}\right) \times \left(\int_0^{\pi} \sin x dx - \frac{1}{2} \int_{\frac{\pi}{6}-\varphi}^{\frac{5\pi}{6}-\varphi} |\sin x| \, dx \right), \quad (45)$$

$$P_{sws} = \frac{1}{2T_{sw}} (E_{\text{swons}} + E_{\text{swoffs}}), \quad (46)$$

where E_{swonn} and E_{swoffn} are the turn on and turn off energy loss of the IGBT at peak current, respectively. Also, E_{swons} and E_{swoffs} are the turn on and turn off energy losses corresponding to the average switching current of the shoot-through state, which is $2i_L/3$.

The Switching Loss Ratio (SLR) for a three-phase Z-source inverter can be obtained as follows:

$$\text{SLR} = \text{SLR}_n + \text{SLR}_s = \frac{P_{swn}}{E_{\text{swonn}} + E_{\text{swoffn}}} + \frac{P_{sws}}{E_{\text{swons}} + E_{\text{swoffs}}}, \quad (47)$$

where SLR_n and SLR_s are the switching loss ratio of each IGBT during non-shoot-through and shoot-through states, respectively.

Therefore, by substituting Eqs. (45) and (46) into Eq. (47), the switching loss ratio can be further expressed as:

$$\text{SLR} = \frac{1}{2T_{sw}} \left(1 + \frac{1}{\pi} \left(\int_0^{\pi} \sin x dx - \frac{1}{2} \int_{\frac{\pi}{6}-\varphi}^{\frac{5\pi}{6}-\varphi} |\sin x| \, dx \right) \right). \quad (48)$$

As can be derived from Eq. (48), a change in parameters, such as T_{sw} and φ, has a significant impact on SLR.

7. Simulation results

In this section, simulation results are given to confirm the proposed analysis of the main formulas of the Z-source inverter. For this purpose, a three-phase Z-source inverter is studied, whose constant parameters are listed in Table 1.

Figure 5(a) and (b) show the voltage stresses across the Z-source capacitor and switching devices, respectively. In these figures, it can be seen that S_C and S_S are approximately boosted to 342 V and 536 V, respectively. These two values are quite close to theoretical values.

Table 1. List of constant parameters and their values.

Parameter	Value	Parameter	Value
V_{dc} (V)	150	V_{ca}	1
R_l (Ω)	30	V_p	0.64
L (H)	160×10^{-6}	M	0.64
C (F)	1000×10^{-6}	T_{sw} (s)	9.83×10^{-5}
φ (rad)	6.66×10^{-5}	f_{sw} (Hz)	10.17×10^{3}

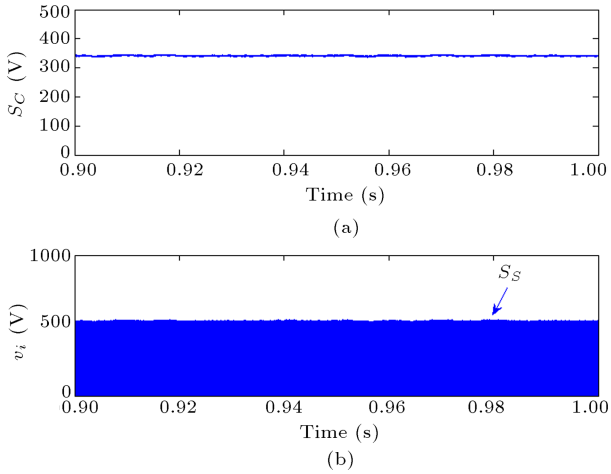

Figure 5. Simulated waveforms of voltage stresses across the (a) Z-source capacitor, and (b) switching devices.

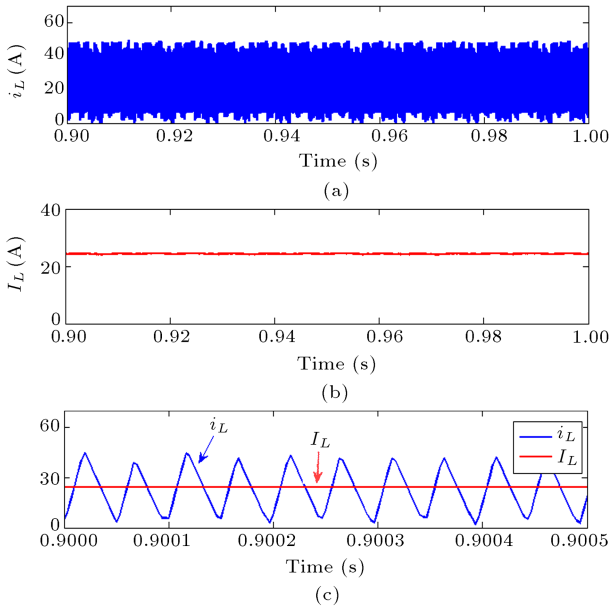

Figure 6. Simulated waveforms of the (a) Z-source inductor current, (b) Z-source average inductor current, and (c) Z-source inductor current with details.

Figure 6 shows the Z-source inductor current i_L and its average value, I_L. As indicated by this figure, I_L is approximately equal to 25 A, perfectly close to the theoretical value.

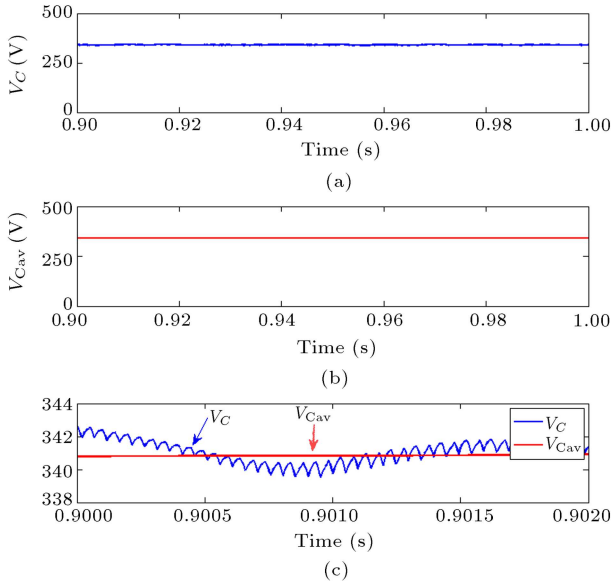

Figure 7. Simulated waveforms of the (a) Z-source capacitor voltage, (b) Z-source average capacitor voltage, and (c) Z-source capacitor voltage with details.

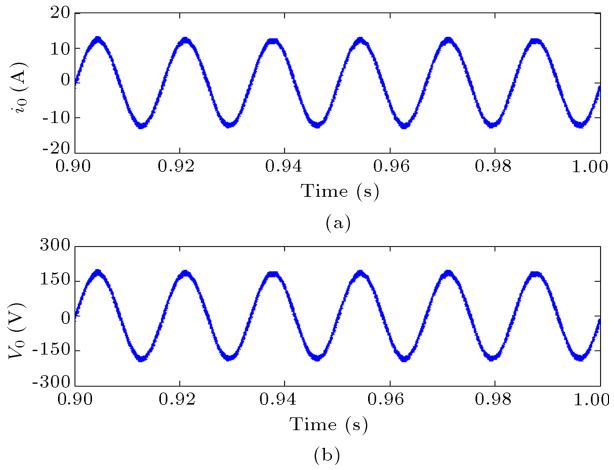

Figure 8. Simulated waveforms of the (a) output phase current, and (b) output phase voltage, for the Z-source inverter.

As indicated by the simulation results in Figure 7, the voltage ripple across the capacitors is very low, and, therefore, the Z-source capacitor voltage, V_C, and its average value, V_{Cav}, are quite close to each other. On the other hand, V_{Cav} is boosted to 341 V, perfectly matching the theoretical value.

Figure 8(a) and (b) show the filtered output phase current and voltage of the Z-source inverter, i_o and v_o, respectively. It is clear that i_o and v_o are perfectly consistent with theoretical values.

8. Conclusion

In this paper, an analysis on the calculation of the main formulas of a Z-source inverter has been proposed. The formulas of the inductor current ripple, capacitor voltage ripple, voltage stress on the devices and capacitors, switching device power and switching loss have been computed. Calculating these formulas will greatly help in improving the performance of the Z-source inverter. Simulation results have also been presented which are perfectly consistent with theoretical values, and this compatibility between theoretical and simulation results has validated the analysis.

References

1. Peng, F.Z. "Z-source inverter", *IEEE Transactions on Industry Applications*, **39**(2), pp. 504-510 (2003).
2. Shen, M., Joseph, A., Wang, J., Peng, F.Z. et al. "Comparison of traditional inverters and Z-source inverter for fuel cell vehicles", *IEEE Transactions on Power Electronics*, **22**(4), pp. 1453-1463 (2007).
3. Peng, F.Z., Joseph, A., Wang, J., Shen, M. et al. "Z-source inverter for motor drives", *IEEE Transactions on Power Electronics*, **20**(4), pp. 857-863 (2005).
4. Hanif, M., Basu, M. and Gaughan, K. "Understanding the operation of a Z-source inverter for photovoltaic application with a design example", *IET Power Electronics*, **4**(3), pp. 278-287 (2011).
5. Bradaschia, F., Cavalcanti, M.C., Ferraz, P.E., Neves, F.A. et al. "Modulation for three-phase transformerless Z-source inverter to reduce leakage currents in photovoltaic systems", *IEEE Transactions on Industrial Electronics*, **58**(12), pp. 5385-5395 (2011).
6. Peng, F.Z., Shen, M. and Holland, K. "Application of Z-source inverter for traction drive of fuel cell-battery hybrid electric vehicles", *IEEE Transactions on Power Electronics*, **22**(3), pp. 1054-1061 (2007).
7. Tang, Y., Xie, S., Zhang, C. and Xu, Z. "Improved Z-source inverter with reduced Z-source capacitor voltage stress and soft-start capability", *IEEE Transactions on Power Electronics*, **24**(2), pp. 409-415 (2009).
8. Shen, M., Wang, J., Joseph, A., Peng, F.Z. et al. "Constant boost control of the Z-source inverter to minimize current ripple and voltage stress", *IEEE Transactions on Industry Applications*, **42**(3), pp. 770-778 (2006).
9. Tang, Y., Xie, S. and Ding, J. "Pulse width modulation of Z-source inverters with minimum inductor current ripple", *IEEE Transactions on Industrial Electronics*, **61**(1), pp. 98-106 (2014).
10. Peng, F.Z., Shen, M. and Qian, Z. "Maximum boost control of the Z-source inverter", *IEEE Transactions on Power Electronics*, **20**(4), pp. 833-838 (2005).
11. Liu, J., Hu, J. and Xu, L. "Dynamic modeling and analysis of z source converter-derivation of Ac small signal model and design-oriented analysis", *IEEE Transactions on Power Electronics*, **22**(5), pp. 1786-1796 (2007).

Biographies

Mohsen Shid Pilehvar received a BS degree in Electrical Engineering from Ferdowsi University, Mashhad, Iran, in 2011, and an MS degree in the same subject from Shiraz University of Technology, Shiraz, Iran, in 2013. His research interests include power electronics, Z-source inverter, multilevel inverters, and application of power electronics in renewable energy systems.

Mohammad Mardaneh received a BS degree in Electrical Engineering from Shiraz University, Iran, in 2002, and MS and PhD degrees in the same subject from Amirkabir University of Technology, Tehran, Iran, in 2004 and 2008, respectively. He has been Assistant Professor at Shiraz University of Technology, Shiraz, Iran, since 2008. His research interests include modeling, design and control of electrical machines and application of power electronics in renewable energy systems and distribution networks.

Amirhossein Rajaei was born in Jahrom, Iran. He received MS and PhD degrees in Electrical Engineering from Tarbiat Modares University, Tehran, Iran, in 2009 and 2013, respectively. He is currently Assistant Professor at Shiraz University of Technology, Shiraz, Iran. His main research interests include renewable energy resources, power converters, electric vehicles, and motor drive systems.